Nat Hazards (2017) 88:1347–1372
DOI 10.1007/s11069-017-2927-y

ORIGINAL PAPER

Agent-based tsunami evacuation modeling of unplanned network disruptions for evidence-driven resource allocation and retrofitting strategies

Alireza Mostafizi[1] · Haizhong Wang[1] · Dan Cox[1] · Lori A. Cramer[2] · Shangjia Dong[1]

Received: 1 January 2017 / Accepted: 10 May 2017 / Published online: 26 May 2017

Abstract The M9 Cascadia subduction zone earthquake represents one of the most pressing natural hazard threats in the Pacific Northwest of the USA with an astonishing high 7–12% chance of occurrence by 2060, mirroring the 2011 devastating earthquake and tsunami in Japan. Yet this region, like many other coastal communities, is underprepared, lacking a comprehensive understanding of unplanned network disruptions as a key component to disaster management planning and infrastructure resilience. The goals of this paper are twofold: (1) to conduct a network vulnerability assessment to systematically characterize the importance of each link's contribution to the overall network resilience, with specific emphasis on identifying the most critical set of links and (2) to create an evidence-driven retrofitting resource allocation framework by quantifying the impacts of unplanned network disruptions to the critical links on network resilience and retrofitting planning. This research used the city of Seaside on the Oregon coast as a study site to create the agent-based tsunami evacuation modeling and simulation platform with an explicit focus on the transportation network. The results indicated that (1) the network bridges are not equally important and some of the critical links are counterintuitive and (2) the diverse ways of spending the limited retrofitting resources can generate dramatically different life safety outcomes. These results strongly suggest that accurate characterization

✉ Haizhong Wang
Haizhong.Wang@oregonstate.edu

Alireza Mostafizi
mostafia@oregonstate.edu

Dan Cox
Dan.Cox@oregonstate.edu

Lori A. Cramer
lcramer@oregonstate.edu

Shangjia Dong
dongs@oregonstate.edu

[1] School of Civil and Construction Engineering, Oregon State University, Corvallis, OR 97331, USA

[2] School of Public Policy, Oregon State University, Corvallis, OR 97331, USA

and measurement of infrastructure network failures will provide evidence-driven retrofitting planning strategies and inform resource allocations that enhance network resilience.

Keywords Unplanned network disruption · Agent-based tsunami evacuation modeling · Evidence-driven resource allocation · Retrofitting planning · Community resilience

1 Introduction

Natural disasters could result in unnecessary loss of life and disproportionate suffering to families and communities if the essential infrastructure systems are not resilient. The Pacific Northwest region is highly prone to a M9 CSZ earthquake (Goldfinger et al. 2012) and near-field tsunami (20–40 min of lead time) mirroring the devastating 2011 Tohoku event in Japan. Yet this region is grossly underprepared for the "Big One" (Schulz 2015a, b), lacking the developed disaster management plans and critical infrastructure it needs to be resilient. Transportation networks are one of the most critical components of the civil infrastructure system susceptible to natural disasters (Murray-Tuite 2007). The performance of a transportation network is essential to emergency responses and recovery activities following an immediate earthquake. Depending on the magnitude and duration of an earthquake, the transportation network typically suffers from certain levels of mobility losses (e.g., bridge failures and road blockage) caused by either ground shaking, or secondary hazards such as landslides or rockfalls triggered by the initial shake. Bridges in transportation networks, specifically, are "critical" and vital to normal and emergency operations. However, they are continuously deteriorating over time and are particularly vulnerable to seismic hazards (Chang et al. 2012). It is critical that bridges retain their traffic-carrying capacities after a devastating earthquake so that people can efficiently evacuate to safer areas. Retrofitting existing bridges is a widely accepted and relatively economical way to enhance bridges' performance against earthquakes and mitigate their functional loss (Chang et al. 2012). Nevertheless, it is neither practical nor economical to retrofit all existing bridges due to budget constraints. In addition, the amount and level of retrofitting are of great significance. Therefore, it is vital to prioritize the bridges' retrofitting with an appropriate strategy. Besides bridges, maintenance of some of the transportation links is also of significance. The criticality of any specific link or bridge is reinforced by the lack of alternative links in an evacuation scenario. Since life safety is the most important measure to evaluate the success of a near-field tsunami evacuation, exploring the effect of network disruption through evacuation mortality would provide an innovative and straightforward perspective to prioritize a retrofitting strategy in a way to minimize the mortality rate considering limited resources.

1.1 Motivation and contribution

The major contributions of this research are (1) an agent-based modeling framework to systematically characterize each transportation link's contribution to the overall life safety and network resilience measured by their contribution to the mortality rate and (2) an evidence-driven retrofitting framework to prioritize resource allocations for maximum life safety benefits. This research integrates the unplanned transportation network disruption

uncertainties into a multimodal agent-based evacuation model to assess the impacts of disruptions considering an agent's choice of evacuation modes (i.e., driving, walking on foot) and their life safety from a network-wide perspective. An innovative agent-based modeling framework is used to identify and classify the criticality of network links, based on their failure impact on the mortality rate of the evacuation, and further, the framework is used to devise the optimal retrofitting plan for the critical links of the network. Research results will enlighten policy makers, city planners, and government officials on how link disruptions (i.e., bridge failures) can affect the evacuees' rerouting decision-making behavior. Ultimately, the efficiency of the evacuation process is analyzed in order to devise a logical retrofitting plan for critical links of the transportation network and rationally allocate the limited retrofitting resources. Using the city of Seaside as a case study, an optimal retrofitting plan is created to prioritize the limited resources to minimize the fatality rate.

1.2 Paper organization

This paper is organized as follows: Sect. 2 presents a brief literature review on planned and unplanned network disruptions. Section 3 details the different critical components of the agent-based modeling and simulation framework. A description of the case study site is provided in Sect. 3.1. Section 4 presents a detailed experiment design and analysis of results. Finally, Sect. 5 summarizes the research and discusses the major findings from this study.

2 Literature review

Most of the existing network disruption (Sullivan et al. 2009) research focuses on traffic flow pattern change (He and Liu 2012; Xie and Levinson 2011), congestion-induced capacity reduction (Sullivan et al. 2010), economic loss estimation (Tatano and Tsuchiya 2008), and rerouting behavior (Qian and Zhang 2013) as a result of the planned disruption (Konduri et al. 2013; Zhu and Levinson 2012). Less work has been done on the impacts of unplanned disruptions to network-wide resilience (Jenelius et al. 2010). Despite methodological advancements, challenges remain in measuring and quantifying the impacts of network disruptions from a network science perspective by characterizing each link's contribution to the overall network resilience (Scott et al. 2006). The lack of a systematic characterization of network resilience hinders understanding how limited retrofitting resources should be allocated to generate maximum mobility and safety benefits for post-disaster response and recovery. This methodological shortcoming is linked with the shortage of empirical data on network failure modes or partial failure/function for a collection of nodes or links in the network (Fessel et al. 2014).

2.1 Planned and unplanned network disruptions

Network disruptions refer to a series of events that change the regular flow of traffic on one or more roadway facilities. Generally, network disruptions are classified as planned and unplanned events. Planned disruptions include traffic congestion or road or ramp closures to accommodate work zones along a freeway segment or bridge section, or to accommodate transit strikes, etc. (Konduri et al. 2013; Zhu and Levinson 2012). Unplanned

disruptions include natural disasters (e.g., tsunamis, earthquakes, floods, landslides, hurricanes), terrorist attacks (e.g., September 11, 2001), infrastructure failures (e.g., I-35W bridge collapse in 2007), severe accidents, etc. (Zhu and Levinson 2012; Jenelius et al. 2010). Network disruptions lead to a drop in capacity on the roadway segment where the incident occurs and result in delays, built-up queues, and spill-backs on to surrounding areas in the network (Konduri et al. 2013). A partial decrease or complete loss of capacity on a road or bridge link can result in travel time increase and changes in travel behavior through congestion and queues. Empirical evidence shows that a majority of unplanned transport network disruptions are followed by "a time-on the order of days or weeks-of uncertainty, learning and adaptation for the travelers" (Jenelius et al. 2010). If the network disruption lasts for a long time, the traffic eventually reaches a new equilibrium, where travelers collect sufficient information and change their travel behaviors accordingly. In such cases, unplanned disruptions have similar impacts to traffic as planned disruptions, as people are more informed and have time to change travel decisions; most common are changes to departure time and route choice (Jenelius et al. 2010). However, the immediacy of an evacuation would leave no room for adaptation. Various approaches have been proposed to model the network disruptions, including static analysis (Earnest 2011), equilibrium analysis (Miller et al. 1999), weighted network model (Earnest 2011), disruption index (Murray-Tuite and Mahmassani 2005; Rahimian and Mcneil 2012), agent-based models (Earnest 2011), damage index (Rahimian and Mcneil 2012), probability model (Chang et al. 2012), and travel time analysis (Bocchini and Frangopol 2010).

2.2 Measures of network disruptions

When it comes to emergency response or disaster evacuation, a system performance metric is required to assess the serviceability of a road network and compare the effectiveness resulting from different intervention or mitigation projects. Such system metrics for road networks can be divided into three categories: (1) connectivity, (2) travel delay cost, and (3) network flow capacity (Chang et al. 2012). Connectivity relies highly on the connectedness of a transportation network. However, it ignores traffic systems' capacities, travel time, and trip length. Travel delay cost has been widely adopted to assess the seismic risk of transportation systems (Kiremidjian et al. 2007). Nevertheless, it is heavily dependent on origin–destination (OD) demand matrices. Network flow capacity metric falls in between: it evaluates the serviceability of transportation networks under specifically determined seismic damage and does not require detailed OD demand information or traveler behavior to compute the travel delay cost. It serves better to evaluate the emergency serviceability of a transportation network in terms of immediate population evacuation. Berdica (2002) defined the vulnerability as "a susceptibility to incidents that can result in considerable reductions in road network serviceability." The serviceability of a link is defined as "the possibility to use that link during a given time period." However, previous research did not examine the availability of alternative links for a specific link in the transportation network. In addition, Jenelius et al. (2006) defined two concepts of criticality and exposure for elements in the network in case of a hazard. The proposed concepts are purely based on the characteristics of the network and not the type and dynamics of the hazard. Therefore, the criticality calculated for any element might not properly reflect the importance of that element's failure.

Moreover, it is vital to know the details of the impacts of the system disruption, for example where events are most likely to happen, and where impacts would be the most severe (Jenelius and Mattsson 2012). The desire to better understand the impacts of

network disruptions has led to a rich body of research. This literature can be classified into two categories: (1) measuring the change of activity–travel behavior in response to network perturbation and user information provision and (2) tool development for simulating network disruptions and evaluating various policies and solutions to alleviate the impacts of network disruptions (Konduri et al. 2013). Zhu et al. (2010) investigated the impact of the collapse of the I-35W bridge over the Mississippi River on regional traffic flow and travel behavior patterns. Akiyama et al. (2012) proposed a probability assessment of bridge performance by estimating bridge failure likelihood through bridge fragility curves.

As Murray-Tuite (2007) stated, "before planning network improvement, they should examine the degree to which the disruption of a link, or set of links, will influence network connectivity." Network connectivity plays a significant part in the performance of the network, especially during an evacuation. However, the connectivity of a network does not necessarily represent the proficiency of the network in an evacuation situation. A transportation network has hundreds of thousand links, and the impact of their failure to the evacuation varies. Identifying which link is critical to the evacuation performance is challenging but meaningful. Existing studies select the critical links based on a travel performance measurement, such as travel time, travel delay, capacity. However, during an evacuation, life safety is of the most concern. Therefore, in this research, the critical link is determined by studying the mortality rate before and after the link failure.

3 Methodology: agent-based tsunami evacuation modeling (ABTEM) framework

The agent-based modeling and simulation framework is coded in NetLogo to evaluate the near-field tsunami evacuation under transportation network disruptions (Wang et al. 2016). NetLogo is a high-level integrated modeling platform through an agent-based programming language (Wilensky 1999). This modeling framework enables the multi-parameter exploration for an emergent phenomenon in a multi-agent system and visualizes the dynamic (time-dependent) scenarios (Railsback et al. 2006). This feature has turned NetLogo into an increasingly popular tool for research due to its extensive documentation, user-friendly interface, expandable modeling environment, the existence of good tutorials, and a large library of preexisting models (Wilensky 1999; Klugl and Bazzan 2012). The major part of complexity in evacuation modeling is largely driven by interactions between agents that capture the emergent behavior of the whole system (Pan et al. 2007). Along with these benefits, the GIS compatibility in NetLogo further validates the use of this platform for modeling and simulating the evacuation dynamics at a community scale, ranging from engineering studies to sociology (Wang et al. 2016). Figure 1 shows a snapshot of the simulation environment coded in NetLogo. As shown in Fig. 1, blue shade illustrates the tsunami wave, and darker blue represents higher waves. Red dots represent the evacuees who were caught by the tsunami inundation, and the orange dots represent the evacuees who are on the way toward the shelters. Yellow circles represent the locations of primary evacuation shelters, and green represents the evacuees who are safely evacuated to one of the safe areas.

It is noteworthy that the simulation we developed only focuses on the consequences of the tsunami hazard, and we do not include direct consequences of the earthquake on the population or the constructed environment. This is a reasonable assumption since over 90% of the loss of life in the 2011 Tohoku disaster was attributed to the tsunami inundation, not

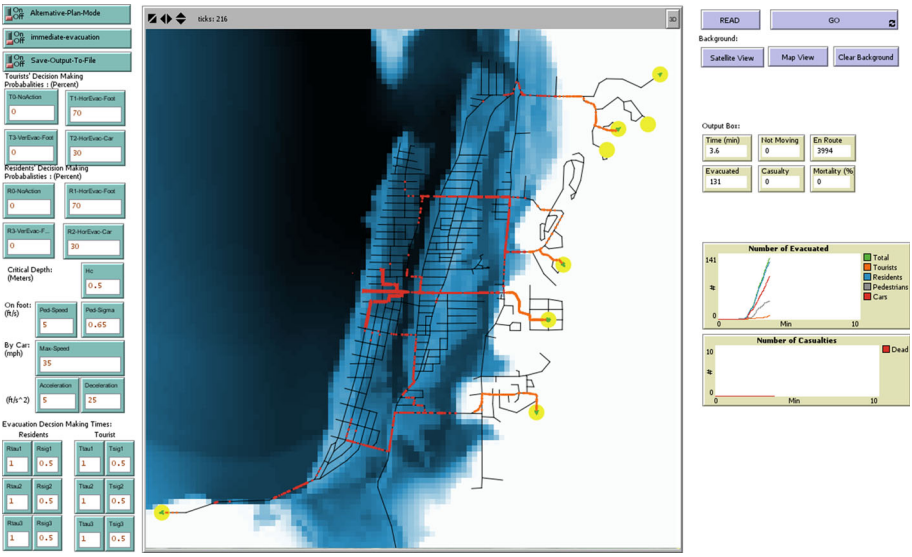

Fig. 1 The interface of the agent-based tsunami evacuation model (ABTEM) for city of Seaside, Oregon, in NetLogo. On the *left panel*, there are the adjustable variables of the simulation, including the tsunami severity, evacuation mode split, behavioral and physical aspects of the evacuee community that possibly affects the mortality rate of the evacuation scenario. The dynamics of the evacuation can be monitored through simulated graphics in the middle which reflects the movement of cars and pedestrians through the network, as well as the dynamics of the inundation wave. The darkness of the *blue color* represents the water level of the inundated area. Throughout the simulation, *dot* represents pedestrians and triangles represent cars. The *red dots* reflect the geographical distribution of the casualties, while the *green dots* show the safely evacuated agents into the designated shelters, shown as *yellow circles*. *Orange dots* are evacuees who are moving toward the safe zones. On the *right panel*, there are the temporal results of the simulation, including the number of casualties, number of safely evacuated, based on the evacuation mode

the preceding earthquake. The ABTEM platform can be extended to a multi-hazard model in future work. For the agent behavior, it is assumed that all agents are autonomous and heterogeneous and that their choices are directly influenced by their surrounding environment and also through interactions. To simplify the problem, it is assumed that agents do not change their mode choice decisions throughout the evacuation, that is to say, an agent who starts evacuating by car will not switch to evacuation on foot, and vice versa. For the sake of network disruption assessment, it is assumed all agents decide to evacuate, although previous experiences have shown that a small portion of people chose to stay (Mas et al. 2011, 2012; Mas and Koshimura 2012).

3.1 Study area and multi-hazard scenario

This study uses the city of Seaside on the Oregon coast which is one of the most vulnerable communities to a combined CSZ earthquake and near-field tsunami (Gonzalez et al. 2009; Wang et al. 2016; Priest et al. 2016). The city of Seaside has recently been the topic of several studies regarding tsunami evacuation as well as seismic resiliency and vulnerability, mainly due to its location and its topography which makes it highly prone to a CSZ tsunami (Wood 2007; Wood and Schmidtlein 2012, 2013; Wood et al. 2016; Priest et al. 2016). This is due, in part, to the proximity to the CSZ, fairly flat topography, and the location of the tsunami shelter areas at more than 1.5 Km from the shoreline. Two rivers,

flowing from south to north, divide the city into three parts. The presence of ten bridges in total, spanning these two rivers, makes multimodal evacuation more complex and highly vulnerable and makes Seaside an interesting case study for further analysis on the effects of a network disruption on the success rate of tsunami evacuation and mortality rates. The current tsunami evacuation plan for the area calls for horizontal evacuation on foot, and the option of vertical evacuation has only been discussed in recent years as a possible option. No comprehensive studies exist which explore the feasibility of vertical evacuation. In addition to Seaside, there are several other towns along the coast with a high risk of near-field tsunamis, including Ocean Shores, WA, and Long Beach, WA (Wood and Schmidtlein 2013).

The CSZ measures 1000 Km in length and extends from the Mendocino Ridge off the coast of northern California to northern Vancouver Island, British Columbia (Venturato et al. 2007; Goldfinger et al. 2012). A near-field event generated from the CSZ is expected to cause widespread damage to the northwest Pacific coast of North America with the first waves arriving in the tens of minutes (Park et al. 2012; Wood and Schmidtlein 2013; Wang et al. 2016). The last great CSZ event occurred more than three centuries ago on January 26, 1700, and was a full-length rupture (Satake et al. 2003). The event is estimated to have had a moment magnitude (M_W) between 8.7 and 9.2, and a slip of 19 m (Satake et al. 2003). The average recurrence interval between full-length CSZ events is 530 years, and the next event is estimated to have a 7–12% probability of occurrence by 2060 (Goldfinger et al. 2012).

3.2 Model behavior overview

Figure 2 shows an example of the model simulation starting with time $t = 0$ representing the end of the initial shaking due to the earthquake to the end of evacuation scenario. For this simulation, it is assumed that no evacuation takes place during the earthquake itself. Figure 2a shows the initial population, shown with brown color, which is distributed normally around the centroid of the beach and downtown area. The agents have the options to evacuate either on foot or by car. Agents change color and shape depending on their mode of transportation Fig. 2b, c. Blue color represents the cars, and orange represents the pedestrians. Figure 2b shows $t = 10$ after the end of earthquake that most of the evacuees have started their evacuation. However, there are many agents who have delayed and they are still in the beach area. Looking at Fig. 2c, d, after approximately 30–35 min the first waves of tsunami reach the shore. Figure 2e shows the first fatalities that occur when the inundation level exceed 0.5 m, represented as agents with red color. It can also be seen that the tsunami has inundated the first part of Seaside after 40 min, crossing the Necanicum River. Finally, the tsunami reaches the runup limit approximately 1 Km inland, 15 min after reaching the shoreline (Fig. 2f). At the end of each simulation, the mortality rate of the evacuees can be calculated and be used as a measurement of effectiveness.

3.3 Monte Carlo simulation

To capture the stochasticity of the simulations, mostly due to the distribution of evacuees with different decision-making parameters and walking speeds, Monte Carlo simulation has been implemented in NetLogo and R, bridging the gap using package "RNetLogo"[1] in

[1] https://cran.r-project.org/web/packages/RNetLogo/index.html.

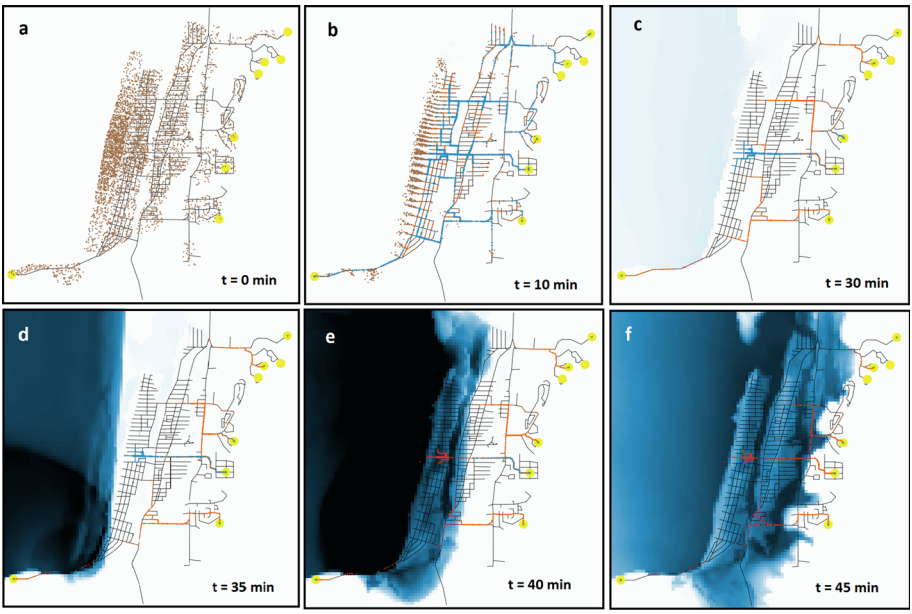

Fig. 2 Snapshots of ABTEM simulation at varying time from the initial start (**a**) to the full inundation (**e**). **a** Shows the initial population distribution which is highly concentrated around the beach and downtown area. **b** Shows partial initiation of evacuation by the community due to different evacuation milling times. *Blue color* represents the vehicles, and *orange color* is assigned to pedestrians. After 30 min (**c**), first waves hit the shoreline, and after 35 min (**d**), it starts to actually inundate the city. **e**, **f** show the movement and dynamics of tsunami wave and the way it inundates the city considering its topography

R. RNetLogo is an open-source package that delivers either a headless interface or a GUI to use NetLogo in R. It provides the functions to run models, execute commands, and push or get values from NetLogo directly in R. It allows the modeler to virtually and systematically control NetLogo using R code. The package has been thoroughly documented, providing the opportunity to run simulations, store the results, and analyze using powerful statistical tools in R (Thiele et al. 2012; Thiele 2014). Our studies show that the average mortality rate of 10 repetitions is fairly close to 100 repetitions. Figure 3 illustrates the variation in mortality rate and the mean mortality rate for two different cases with 100% cars and 100% pedestrians. Results indicate that the difference in the mean mortality rate between 10 and 100 repetitions, for both cases, is less than 0.1%. Therefore, the assessments have been done using a Monte Carlo simulation mostly with 10 times repetition for computational benefits in this study but the number of repetitions could be set as 100 or 1000 in future endeavors.

3.4 Model components

There are essentially five building blocks of the model: population distribution, road network, tsunami inundation data, the locations of evacuation shelters, and casualty model, each of which is explained in detail below.

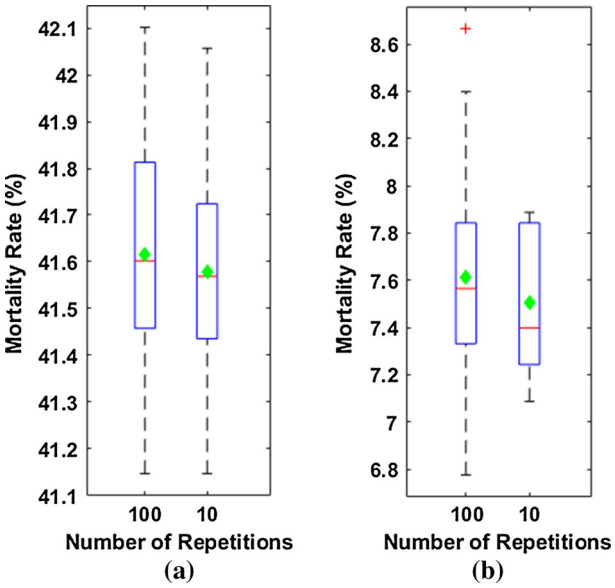

Fig. 3 Mortality rate variations for 10 and 100 number of repetitions. *Red line* represents the median mortality rate, and the green diamond represents the average mortality rate. **a** 100% car, **b** 100% pedestrian

3.4.1 Population distribution model

In the model, the worst-case scenario, noontime of a weekend in the summer, is considered. Tourists and residents are distributed unevenly based on the attributes of the environment (i.e., tourist attractions and residential areas) to the 38 areas shown in Fig. 4a.

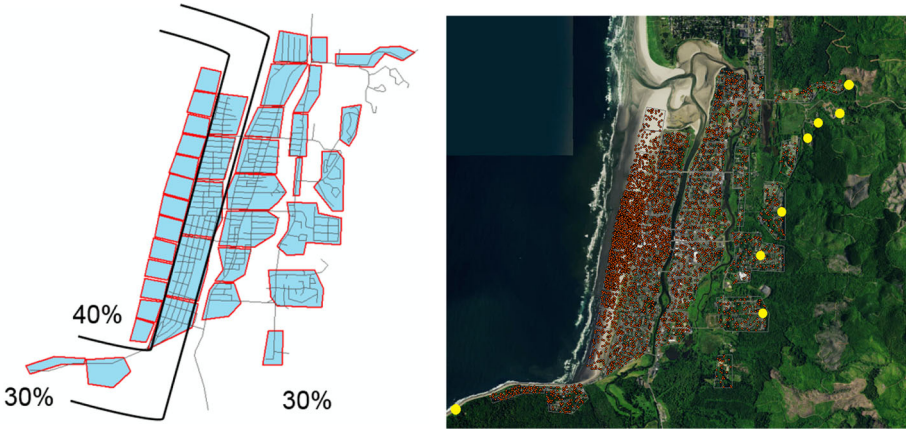

Fig. 4 Population distribution for city of Seaside, Oregon, including residents and tourists. **a** shows the arbitrary distribution of the population which reflects the worst-case scenario with high level of population, 40% in this case, along the shoreline. The population on the shoreline is normally distributed around the centroid of the beach, as shown in (**b**). Other than this, 30% of the population is distributed normally to the downtown area. The rest of the population is distributed uniformly to the residential area

These areas are chosen such that the change in land use and other attributes is minimal in each region. As shown in Fig. 4b, the population is normally distributed around the centroid of the beach and the downtown area. Therefore, the concentration of the evacuees in those two areas is high. Moreover, although different categories of people (i.e., residents and tourists) may respond differently to the same hazard, categorization of the evacuees based on their attributes should be considered for a realistic evacuation simulation platform. For the sake of the main objective of this study it is assumed that different categories react to the hazard in the same fashion. That is, the agents choose their destination, their route, their mode of transportation, and immediacy of evacuation regardless of their knowledge and familiarity with the area.

According to US Census data, the latest population of the city of Seaside is estimated to be 6445 with 20% under the age of 18.[2] The number of tourists in the city considering the amount of rentals, hotels, and inns can be up to 10,000 on any given day. However, due to computational challenges in NetLogo coming from agent-agent interactions, 4500 evacuees have been included in the simulation runs. For the purpose of network assessment, the number of agents is valid, as it allows for relative comparison regarding the sensitivity of the mortality rate to the influential factors. We believe that the relative criticality of the links remains stable. It is not anticipated that increasing the number of evacuees in the model will significantly alter the outcomes of critical link identification.

3.4.2 Road network

The road network is imported into the model as a GIS shapefile which was extracted from OpenStreetMap[3] with markings for the area of interest. It is assumed that all the agents (i.e., residents and visitors) are to follow this network, including the potential crossing of 10 two-lane bridges. For the purpose of network assessment, the possibility of network disruption in the form of link accessibility, limiting access to (a) neither pedestrians nor cars and (b) pedestrians only is considered. Conservatively, all network links are considered as two-way one-lane streets with a speed limit of 55 km/h. This is a reasonable assumption based on the speed limits (maximum allowable speed) of the area and field observations of the general standing of the network. Refer to Wang et al. (2016) for the details of the interactions of agents with the transportation network.

3.4.3 Tsunami shelters

Oregon Department of Geology and Mineral Industries has proposed eight evacuation shelters outside the inundation zone as shown in Fig. 4b with yellow color (Priest et al. 2013). These are the primary evacuation locations in the model, which are placed outside the inundation zone. Although recently there have been studies regarding the impact of vertical evacuation shelter and how they can reduce the number of casualties (Wood et al. 2014; Wang et al. 2016), for the sake of the main objectives of this study, the focus is on the primary evacuation shelters. All shelters are assumed to have the capacity to fit the evacuees. In addition, it is assumed that all shelters are structurally sound and can withstand tsunami and earthquake forces (FEMA 2008).

[2] http://www.cityofseaside.us/.

[3] http://www.openstreetmap.org.

3.4.4 Tsunami inundation

The tsunami inundation dynamics is generated by the ComMIT/MOST model developed by NOAA calibrated for Cascadia subduction zone (Titov and Gonzalez 1997). Park and Cox (2016) had proposed a probabilistic model for tsunami inundation that incorporates uncertainties associated with the event. However, in this study, inundation is modeled as a definite extreme event with a fixed 2500-year return interval. The inundation model supplies time variation of flow depth and speed for the area of interest. The details of the inundation model can be found in (Wang et al. 2016).

3.4.5 Casualty model

Although calculating the rate of casualties can be highly complicated due to the variability of a person's age, gender, and mental and physical state (Yeh 2010), the casualty model in the simulations is simplified. Many studies have looked into the hydrodynamics of the tsunami and its impact on the human body, considering both speed and height of the flow, using simplified (Lind et al. 2004; Jonkman et al. 2008) as well as detailed models of the body (Koshimura et al. 2006; Muhari et al. 2011). However, in this paper, for computation simplification purposes, only wave height was taken into consideration. It has been assumed that if a wave with a height of H_c or more touches an agent, it will be considered as a casualty. This assumption might not reflect an accurate mortality rate; however, for comparison purposes and assessment of the transportation network, this gives us a reasonable estimate of mortality rate. Besides, H_c can reflect the vulnerability of the evacuee community to the inundation force. For example, in a population with high percentages of elderly and children the vulnerability is high, and therefore, the H_c can be adjusted to lower values. The H_c for these simulations has conservatively been set to be 0.5 m. Model casualties beyond the initial (approximately 1 h) inundation such as hypothermia or heart attack are not modeled.

3.5 Agent decisions

Decision making in emergency situations is a highly complex process. Although Yin et al. (2014) had analyzed the process and its impacts on evacuation travel demand for hurricane evacuation scenario, the characteristics of decision making varies with hazard type. In this study, it has been assumed that human decisions are limited to the following criteria.

3.5.1 Mode choices

Each agent can make one of the following choices. Option 1 is horizontal evacuation on foot. Option 2 is horizontal evacuation by car. It also has to be noted that in order to replicate the worst-case scenario and to expose the transportation network to the highest level of traffic demand, it has been assumed that there is only one person in each vehicle. The probability of choosing an option can be specified by the evacuee group proportions. For example, for a given simulation, the population may have 70% who choose horizontal evacuation on foot (Opt. 1) and 30% who choose horizontal evacuation by car (Opt. 2). Refer to Wang et al. (2016) for the details of decision model.

3.5.2 Milling time

One of the most challenging aspects of modeling natural hazard evacuation, especially for near-field tsunami evacuations with very low preparation time, is to model evacuation milling time. Understanding psychological aspects involved in the process of departure time decision making is complex. It has been shown that milling time has a great impact on both the formation and evolution of bottlenecks and traffic congestion (Naser and Birst 2010), and mortality rate of the evacuation scenario (Wang et al. 2016). To capture the evacuation preparation time, as suggested by Mas et al. (2011), departure times follow a Rayleigh distribution as presented by Wang et al. (2016).

To abstractly consider the decision-making process, values of τ and σ are reasonably calibrated and the milling time is randomly drawn from the mentioned distribution with the following formula (Tweedie et al. 1986; Lindell and Prater 2007).

$$P(t) = \begin{cases} 0 & 0 < t < \tau \\ 1 - e^{-(t-\tau)^2/(2\sigma^2)} & t < \tau \end{cases} \quad (1)$$

where t is the departure time in minutes after earthquake. Both τ and σ can be adjusted in the platform. τ represents the minimum time that an evacuee needs to get prepared, and σ represents the spread of the departure times. The larger the σ is, the larger the tail of the distribution toward later departure times will be. Slight increases in τ and σ will lead to an enormous increase in mortality rates (Wang et al. 2016). For the sake of the main objective and having accurate analysis on the vulnerability of transportation network, and following the suggestion of government officials regarding the importance of immediate evacuation, it is assumed τ to be 1 min and σ to be 0.5, meaning that 99% of agents start their evacuation between 1 to 2 min and 30 s. Refer to Wang et al. (2016) for more information regarding the milling time and its impacts on mortality rate.

3.6 Vehicular movement

The movement of vehicles is governed by the classic car-following model (Brackstone and McDonald 1999), the General Motors model (Chandler et al. 1958; Herman et al. 1959), with the following equation.

$$a_{n+1}^{t+\delta t} = \left[\frac{\alpha_{l,m} \left(v_{n+1}^{t} \right)^{m}}{\left(x_{n}^{t} - x_{n+1}^{t} \right)^{l}} \right] \left(v_{n}^{t} - v_{n+1}^{t} \right) \quad (2)$$

where x_n^t is the location of leading vehicle at time t, v_n^t is the speed of leading vehicle at time t, x_{n+1}^t is the location of following vehicle at time t, v_{n+1}^t is the speed of following vehicle at time t, v_{n+1}^t is the speed of following vehicle at time t, l is the distance headway exponent (varying from -1 to $+4$), m is the speed exponent (varying from -2 to $+2$), $\alpha_{l,m}$ is the sensitivity coefficient, and δt is the perception-reaction time. The parameters are adjustable and can be calibrated using empirical data. Despite the lack of empirical data regarding the driving behavior in emergency situations, the following parameter sets, shown in Table 1, have been chosen to simulate the vehicular movement.

The perception-reaction time is known to be lower than usual in emergency situations since the drivers tend to be more alert and responsive if they are aware of the approaching threat. Therefore, the perception-reaction time in this case, conservatively and in favor of evacuation by car, is assumed to be fairly close to zero. In addition, parameter α is

Table 1 Car-following model parameters

Parameter	Notation	Value
Distance headway exp	l	2
Speed exp	m	0
Perception-reaction time	δt	0
Sensitivity coef	α	0.14

estimated based on the jam density, K_j, of 155 veh/km and free flow speed, V_f, of 55 km/h. In addition, parameter α linearly correlates with the range of accelerations and decelerations calculated from the car-following model. Therefore, it has to vary in a reasonable and realistic manner. Simulations have shown that α of 0.14 leads to accelerations in the range of 1.5–3 m/s^2. Decelerations, on the other hand, vary from 3 to 7.5 m/s^2. Based on the literature, this range of accelerations and decelerations represent the empirical data fairly well, considering the fact that in the case of evacuations, accelerations and decelerations tend to be higher. Therefore, changes in α are not suggested.

It is worth mentioning that the combination of parameters above, with the assumption of steady state traffic flow, from a macroscopic point of view, leads to well-known Greenshields model (Gazis et al. 1961) which represents a linear relationship between speed and density. Figure 5 shows the speed–density diagram generated by the evacuation simulation model. The reproduction of this classic speed–density relationship from the ABTEM simulation further verified the validity of the traffic dynamics. As shown in Fig. 5, speed decreases when density increases. In addition, the graph is highly concentrated around higher densities, which shows that the network is in a congested phase.

3.7 Pedestrian movement

The speed of evacuation is another significant variable governing hazards evacuation (Wood and Schmidtlein 2012). Normal walking speed is on average 1.4 m/s. For the simulation of near-field tsunami evacuation, although people tend to walk faster in emergency situations, the mean walking speed is conservatively set to be 1.2 m/s (Knoblauch et al. 1995). To capture the walking speeds of the elderly, children, and also, fast walkers, it is assumed that walking speeds follow a normal distribution. Conservatively,

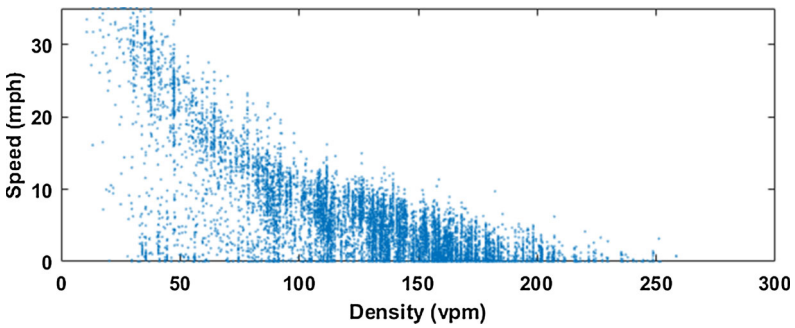

Fig. 5 The speed–density relationship generated from the ABTEM simulation. The simulation results show the congested state of most of the links on the network, as the points are concentrated toward higher densities and lower speeds

the normal distribution's standard deviation is set to 0.2 m/s, which covers very slow walking to slow running, ranging from 0.5 to 1.7 m/s (TRB 2010; Wang et al. 2016). Refer to Wang et al. (2016) for details of the pedestrian movement rules.

4 Experiment design and results

Traditionally, critical link is identified through its contribution to the network travel time. In an evacuation scenario, however, life safety is the first priority. Building upon the agent-based tsunami evacuation platform, an innovative critical link identification method is presented in this section, along with the detailed retrofitting scheme utilized to maximize the benefits of life safety.

4.1 Critical links identification

In this research, the criticality of a link comes from the impact of the failure of the link on life safety, and in particular mortality rates. It is, therefore, essential to identify all the critical links over the investigated transportation network. There are around 700 links within the transportation network of this case study, including bridges, streets, arterials, and highway links. The failure of all links, individually, has been assessed, and the links that had the greatest impact on the mortality rate of evacuation scenario in the transportation network were identified. It is assumed that all the evacuees have prior knowledge regarding any broken links and reroute to their destination accordingly. To capture the variation of different decisions as well as walking speeds, each scenario has been simulated multiple times; the mean mortality of each scenario has been assessed to find critical links in the network. It is worth mentioning that criticality of a link is correlated with the mode choice split. In other words, failure of a link can highly impact the efficiency of evacuation if the evacuees are evacuating on foot, but not in the case where evacuees drive, and vice versa. To account for different splits of evacuation mode, critical links have been identified for 5 different combination of mode splits: (1) 100% pedestrians; (2) 75% pedestrians–25% cars; (3) 50% pedestrians–50% cars; (4) 25% pedestrians–75% cars; and (5) 100% cars.

4.1.1 Critical link selection criteria

Figure 6 shows the normalized increase in mortality rates of a scenario where a specific link is failed, over the average mortality rate of all links failures, for different evacuation mode splits. For example, looking at Fig. 6a, there are 10 links that their failure increases the mean mortality rate by at least 5%. Interestingly, there are a few links that are critical in cases where the majority of evacuees are pedestrians, but not in cases where the percentage of vehicles is high. Analogously, there are a few links that are considered as critical only when the percentage of cars is high. There are several links that are considered in all the evacuation mode splits. Figure 6f shows the average mortality rate increase for each link over all the 5 different evacuation mode splits. In this study, links whose failure causes an increase in mortality rate over 5% are considered as critical, and further assessment has been done on these identified links. The other links are expected to have minimal criticality and do not affect mortality rate dramatically upon failure as multiple alternative routes exist. In the next section, these critical links are mapped to the transportation network of

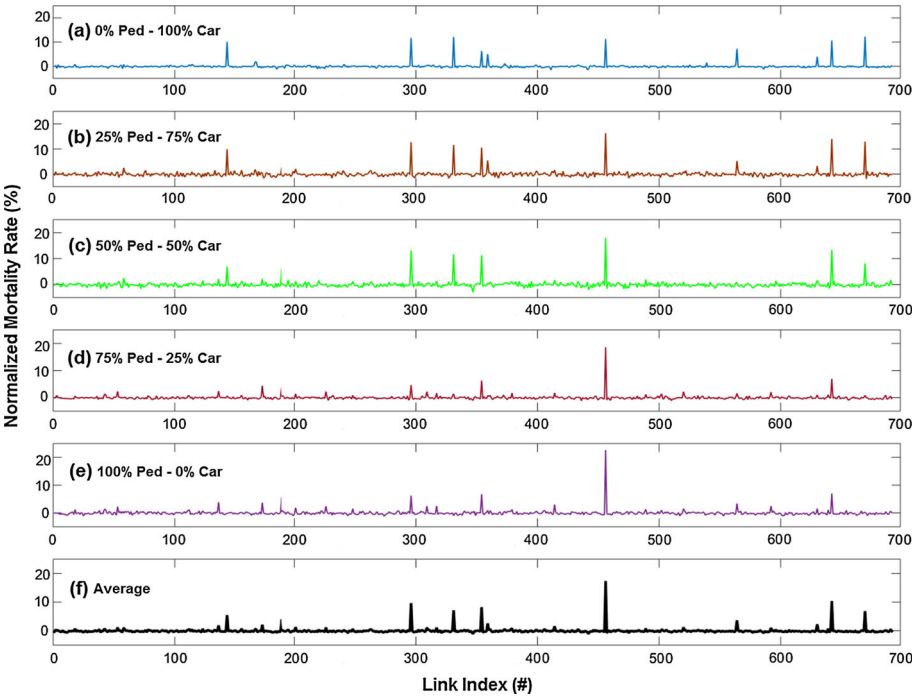

Fig. 6 Normalized mortalities associated with each link's failure. *Y-axis* shows the increase in mortality rate associated with failure of each link, compared to the average mortality rate for each specific evacuation mode split. Therefore, the peaks on this set of graphs redirect to the links whose failure poses massive impact on mortality rate and evacuation efficiency. It can be seen that the collection of critical links varies for different evacuation mode splits. Figure 7 visualizes the critical links for each case

Seaside to find the topographically and structurally vulnerable ones to devise a plan for retrofitting.

4.1.2 Critical links visualization

Figure 8 shows the visualization of the identified critical links in the transportation network of this study for different evacuation mode choice combinations. Surprisingly, not all bridges have large impacts on mortality rates. It can be explained by the potential availability to alternative routes in case of failure. For high percentages of cars, as shown in Fig. 7a, b four main bridges and the roads leading to highly demanded shelters are marked as critical. This is mostly due to the fact that failure of either of these links causes a severe congestion to adjacent links, leading to higher travel times and thus higher fatality rates. As the percentage of vehicles decrease, the links which are adjacent to shelters are no longer marked as critical. Although with the failure of those links, the evacuees are forced to choose another available shelter, the concentration of pedestrians does not have an impact on travel times as it does on vehicles. Therefore, as shown in Fig. 7d which represents the critical links for the evacuation scenario with 75% pedestrians and 25% cars, the critical links are narrowed down to three main bridges and one arterial. The failure of this arterial will cause an isolation to the top left part of the transportation network. For the scenario where all the evacuees decide to evacuate on foot, as in Fig. 7e, the bottom left road and its

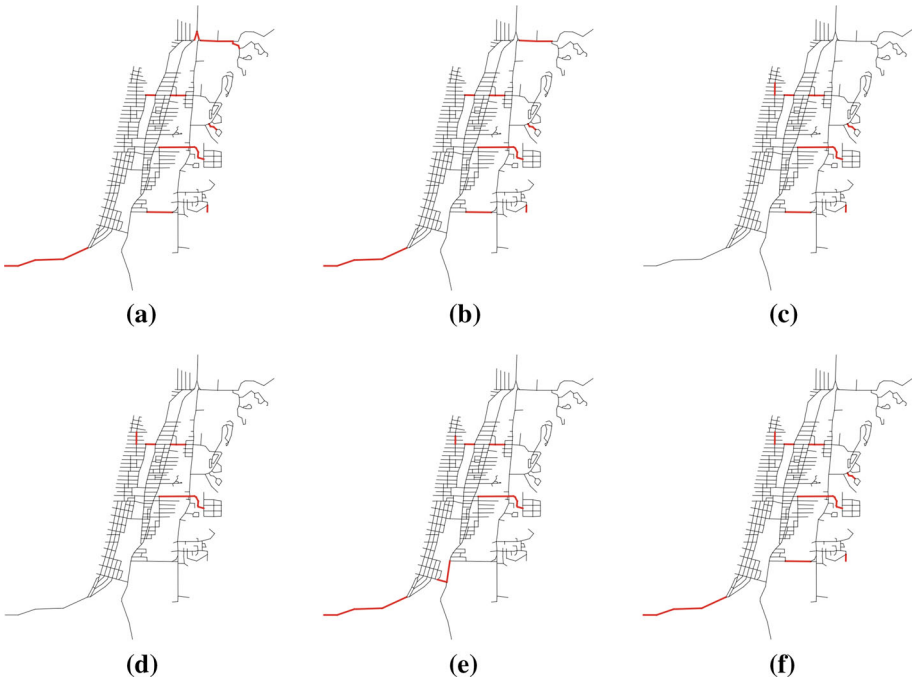

Fig. 7 Color coded network, representing critical links. **a**–**f** show the variation of identified critical links with the evacuation mode choice split, corresponding to Fig. 6. **a**, **b** reflect the scenarios with high percentages of cars. In these cases, bottom left link that acts as an outlet for the evacuees on the south part of the beach proves to be influential. With the increase in percentage of pedestrians to 50 (**c**) and 75 (**d**), moving toward optimal mode choice split, despite emergence of a new set of links that are considered critical only for high percentages of pedestrians, the number of critical links collectively decreases. Moving on to fully on-foot evacuation (**e**), interestingly the number of critical links increases. (**f**) shows that the links that are collectively combining all 5 different mode split cases are considered as critical. **a** 0% Pedestrain–100% cars, **b** 25% pedestrain–75% cars, **c** 50% pedestrain–50% cars, **d** 75% pedestrain–25% cars, **e** 100% pedestrain–0% cars, **f** average

adjacent bridge is added to critical links. These links become critical because their failure leads to a sizable increase in distance to the safe zone for the agents in the lower sections of the beach. Figure 7f illustrates the critical links identified based on the average mortality increase over all the different mode splits.

In total, there are 13 critical links identified in the whole transportation network of Seaside, OR. However, not all of these links have equal impacts on mortality rate in an evacuation. Moreover, running retrofitting planning algorithm on 13 critical links is computationally expensive. Therefore, we have to narrow down the important links to the ones that are either known as being vulnerable or are expected to be influential on fatality rate with higher certainty. Since the four links on the far east side of the city, adjacent to the evacuation shelters, are located outside of the inundation zone, retrofitting them does not seem to be of high priority. In addition, retrofitting arterials, compared to the bridges, is not of great significance since they are expected to be partially functional even facing extreme earthquakes. Furthermore, even though they are closed for vehicles, they probably can still carry pedestrians. One exception, however, is the bottom left road which is highly prone to a landslide after an extreme earthquake. With all this in mind, and accounting for

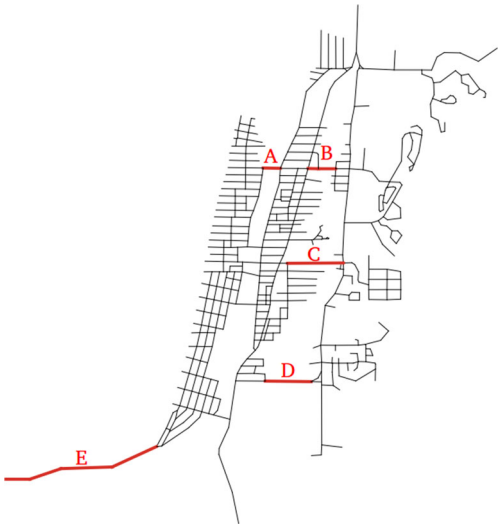

Fig. 8 Final critical links. This subset of critical links has been chosen based on the collective impact that they expose on mortality rate of the evacuation in different scenarios with various evacuation mode split, as well as structural stability and vulnerability. *A*, *B*, *C*, and *D* are bridges that do not have close rerouting alternative in case of failure. *E* is an outlet to one of the important shelters which is prone to landslides in case of earthquake

the insights of the structural engineers regarding the stability and vulnerability of the bridges and other links, there are five links identified for retrofitting purposes, shown in Fig. 8. Further assessment of the degree to which a link is damaged in order to propose an optimal retrofitting plan is provided.

4.2 Retrofitting analysis

In this section, we assess the damage to each of the previously determined critical links. Functionality states to which any transportation facility operates is categorized as follows: (1) able to accommodate both vehicles and pedestrians, *INTACT*, (2) able to accommodate only pedestrians, *PED*, and (3) not able to accommodate any kind of traffic, *FAILED*.

The goal is to prepare a retrofitting plan considering limited resources on the critical links to minimize mortality rates. In order to formulate the problem, a few assumptions have been made regarding the details of the retrofitting. First, if a bridge is not retrofitted, it fails as a consequence of an earthquake. Second, one level retrofitting costs one unit of resources and makes a bridge remain functional for pedestrians after an earthquake. Third, another level of retrofitting costs another *RATIO* number of resources and makes a bridge remain intact after the earthquake, meaning that it will be functional for both pedestrians and vehicles. Therefore, fully retrofitting a bridge costs $RATIO + 1$ number of resources.

Considering the states mentioned, and for different values of *RATIO* and splits of evacuation mode, retrofitting planning is represented in Fig. 9a, b. Besides a detailed retrofitting plan for all the cases, the objective is to find general rules for retrofitting which can be applied to different evacuation cases with different splits and different retrofitting plans with different *RATIO*s. As expected, there are numerous ways to spend the few units of resources to retrofit the system. The aim is to minimize the mortality with respect to constraints on alternatives to spending those amounts of resources. The following section explains a constraint satisfaction problem that clears the limits and alternatives of spending a specific amount of resources.

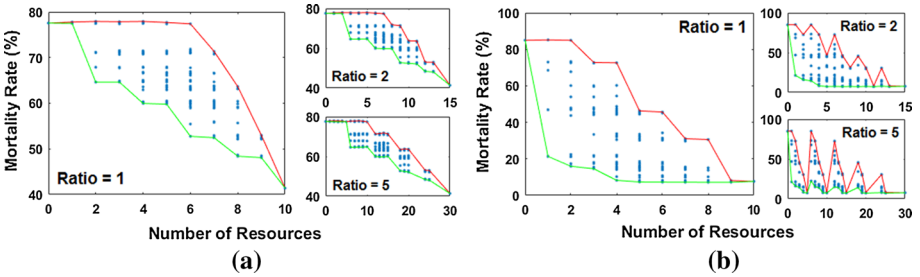

Fig. 9 Retrofitting resources planning—single mode evacuation. Each blue dot corresponds to mortality rate associated with a specific expenditure alternative. The alternative that leads to the lowest mortality rate is the best option for expenditure, and it is represented by the green line. On the other hand, the red line represents the upper bound of spending specific amount resources. **a** associates with the case that all the evacuees evacuate by car. Therefore, retrofitting a link to remain pedestrian accessible has no impact on the mortality rate, and thus, mortality rate constantly decreases with the increase in number of resources. On the other hand, **b** reflects retrofitting scheme for fully on-foot evacuation. Analogously in this case, there is no benefit in retrofitting to the state that the link stays intact after the earthquake. Thus, mortality rate drops at the beginning as the number of resources increases and then stays constant after the point that all the links are retrofitted to *PED* state. **a** 100% car, **b** 100% pedestrian

4.2.1 Constraint satisfaction formulation

These alternatives can be formulated as a constraint satisfaction problem (CSP):

$$N \times 1 + M \times (Ratio + 1) = R \tag{3}$$

$$N + M \leq N_{cr} \tag{4}$$

$$N, M \in \mathbb{N} \tag{5}$$

where N is the number of retrofitted links to be pedestrian accessible (PED), M is the number of retrofitted links to be intact (INTACT), R is the number of resources available, and N_{cr} is the number of critical links which in this case equals to 5 links. The above integer equation can either have no integer answers for N and M or have multiple sets of answers for N and M. After solving the above equation, the number of alternatives ($N_{alternatives}$) to spend R number of resources on $M + N$ bridges can be calculated as following:

$$N_{alternatives} = \sum_{M,N} \binom{N_{cr}}{M+N} \binom{M+N}{M} \tag{6}$$

As shown in the figures, the blue dots represent mean mortality rates associated with the various resource consumption alternatives from retrofitting. For example, if we assume the $RATIO = 2$, and we have $R = 6$ number of resources, considering city of Seaside, with $N_{cr} = 5$ identified critical links, the solutions to Eq. 3 would be the following: (1) $N = 0$ and $M = 2$, retrofitting two bridges to the highest extent (INTACT); and (2) $N = 3$ and $M = 1$, retrofitting one of the bridges to the highest extent (INTACT) and two of the others to be pedestrian accessible (PED). In light of Eq. 6, the number of different alternatives for spending 6 units of resources with the above combination on 5 critical links can be calculated in the following way.

$$N_{alternatives} = \binom{5}{2}\binom{2}{2} + \binom{5}{4}\binom{4}{1} = 10 + 20 = 30$$

As Fig. 9 shows, 30 blue dots for $R = 6$ are plotted which represent the mortality rates associated with 30 different alternatives of spending 6 units of resources.

4.2.2 *Retrofitting scheme*

Figures 9 and 10 represent the expected mortality rate associated with different alternatives of spending different amount of resources, respectively, for single mode and multimodal evacuation scenarios. As stated in the objective, for each specific amount of resources, the alternative that leads to the lowest mortality rate is the best option and it is represented by the green line in the figures. Moreover, the red line represents the upper bound of spending specific resources. In other words, it bounds the worst option of spending a specific amount of resources which results in the highest mortality rate. As before, to capture the stochasticity of the system, each scenario has been simulated multiple times and mean mortality rates were used for assessment. The slopes of green lines between resource units represent the value of the retrofitting in terms of decreasing mortality rates. In other words, this can be translated into a cost–benefit problem in which one considers the cost of retrofitting and consuming resources against the benefit of decreasing the number of fatalities.

Retrofitting, in rare cases, can surprisingly increase the mortality rate. This phenomenon happens mostly due to opening a new route to cars that may result in concentrations of vehicles. In these cases, road closure (e.g., network disruption) will result in dissipation of traffic that leads to lower densities and thus lower travel times. However, the availability of a major route for vehicles might encourage a rebound effect in which additional people decide to use the link, which in turn causes severe congestion and higher travel times.

4.2.2.1 Single mode evacuation Figure 9a shows the retrofitting benefits for the case that none of the evacuees walk and all the population drive to safe zones. In this case, we see that parameter *RATIO* has no impact on the details of retrofitting plans since there are no pedestrians using the network, and thus, retrofitting a bridge to stay pedestrian accessible

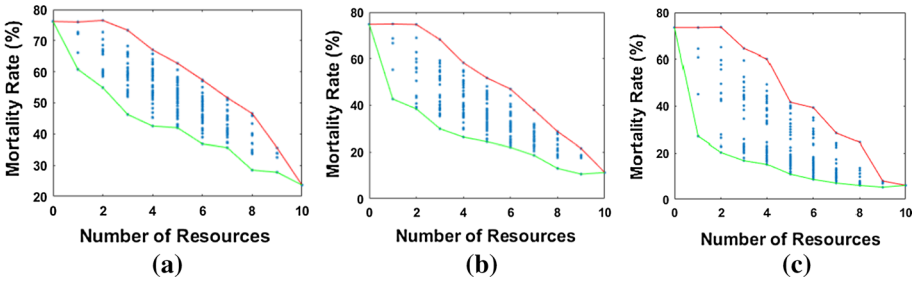

Fig. 10 Retrofitting resources planning—multimodal evacuation. This figure shows the benefits gained on decrease in mortality rate through retrofitting for different multimodal evacuation scenarios, assuming *RATIO* = 1. As expected, comparing Figs. 9 to 10, it can be stated that Fig. 10 covers the spectrum in between 9a and 9b. For high percentages of cars (**a**), the mortality rate almost constantly decreases with the increase in retrofitting. As the percentages of pedestrians increase (**b**, **c**), higher marginal decrease at the beginning of the graph appears. **a** 25% Pedestrain–75% car, **b** 50% Pedestrain–50% car, **c** 75% Pedestrain–25% car

Table 2 Retrofitting plan details—single mode evacuation

Number of retrofitted links	Pedestrian (%)	Critical link					Mortality rate (%)
		A	B	C	D	E	
0 (Baseline)	0	FAILED	FAILED	FAILED	FAILED	FAILED	77.61
	100	FAILED	FAILED	FILED	FAILED	FAILED	85.23
1	0	FAILED	FAILED	FAILED	FAILED	INTACT	64.63
	100	FAILED	FAILED	PED	FAILED	FAILED	21.33
2	0	FAILED	FAILED	INTACT	INTACT	FAILED	59.96
	100	FAILED	FAILED	PED	FAILED	PED	15.93
3	0	FAILED	FAILED	INTACT	INTACT	INTACT	52.74
	100	FAILED	FAILED	PED	PED	PED	14.57
4	0	FAILED	INTACT	INTACT	INTACT	INTACT	48.39
	100	PED	PED	PED	FAILED	PED	8.24
5	0	INTACT	INTACT	INTACT	INTACT	INTACT	41.41
	100	PED	PED	PED	PED	PED	7.33

has no impact on the mortality rate. It can also be seen that retrofitting the first bridge to remain INTACT has the most value and the highest decrease in the mortality rate (13% drop from $\sim$78% to $\sim$65%). Table 2 clarifies the priority of critical links to be retrofitted with the corresponding resultant mortality rate. Looking at the mortality rate column in Table 2, improvement in the mortality rate at each level of retrofitting, compared to the baseline, can be interpreted and mapped to the green lines in Fig. 9.

Figure 9b shows the benefit of retrofitting links in the case that all the evacuees evacuate on foot. Therefore, there would be no benefit in retrofitting a link to remain INTACT since there are no cars using the network. This explains the green curve in the figures to decrease in the beginning and stays the same as the bridges are upgraded to remain INTACT. Like the other single mode evacuation case, retrofitting the first bridge has the most value and decreases the mortality rate by 65%. Regarding the impact of *RATIO* parameter, it does not impact the general trend of the cost–benefit analysis; however, it affects the details of the retrofitting priorities. Table 2 shows the priority of critical links to be retrofitted.

From Table 2, the first link that should be retrofitted, for the case with 100% cars, is Link E which helps to evacuate all the cars that are on the west side of the city and the beach area to the bottom left evacuation shelters. Retrofitting bridge C by itself does not have a significant impact on the mortality rate for cars since it does not provide enough capacity for all the evacuees who are located on the beach to evacuate to the east side shelters. On the other hand, in the case of evacuation on foot, retrofitting bridge C has the higher impact and helps people move to safe zones quicker. The rest of the retrofitting priorities for these two cases can be interpreted by the table.

4.2.2.2 Multimodal evacuation Figure 10 shows the decrease in expected mortality rate when the evacuation is multimodal, assuming $RATIO = 1$. Analogously, it can be interpreted as described in single mode evacuation.

Table 3 presents the retrofitting plan's details for multimodal evacuation with retrofitting $RATIO = 1$. For example, if the retrofitting *RATIO* is equal to 1 and the amount of

Table 3 Retrofitting plan details—multimodal evacuation—*RATIO* = 1

Number of resources	Pedestrian (%)	Critical link					Mortality rate (%)
		A	B	C	D	E	
0 (Baseline)	25	FAILED	FAILED	FAILED	FAILED	FAILED	76.54
	50	FAILED	FAILED	FAILED	FAILED	FAILED	75.12
	75	FAILED	FAILED	FAILED	FAILED	FAILED	73.11
1	25	FAILED	FAILED	PED	FAILED	FAILED	60.76
	50	FAILED	FAILED	PED	FAILED	FAILED	42.70
	75	FAILED	FAILED	PED	FAILED	FAILED	26.86
2	25	FAILED	FAILED	INTACT	FAILED	FAILED	54.90
	50	FAILED	FAILED	INTACT	FAILED	FAILED	38.46
	75	FAILED	FAILED	PED	FAILED	PED	20.22
3	25	FAILED	FAILED	PED	FAILED	INTACT	46.26
	50	FAILED	FAILED	PED	FAILED	INTACT	29.97
	75	FAILED	FAILED	PED	FAILED	INTACT	16.71
4	25	FAILED	FAILED	INTACT	INTACT	FAILED	42.55
	50	FAILED	FAILED	INTACT	INTACT	FAILED	26.37
	75	FAILED	PED	PED	FAILED	INTACT	15.09
5	25	FAILED	FAILED	INTACT	INTACT	PED	41.99
	50	FAILED	INTACT	PED	INTACT	FAILED	24.37
	75	PED	PED	PED	FAILED	INTACT	10.89
6	25	FAILED	FAILED	INTACT	INTACT	INTACT	36.84
	50	PED	INTACT	PED	INTACT	FAILED	22.00
	75	PED	INTACT	PED	INTACT	FAILED	8.62
7	25	FAILED	INTACT	PED	INTACT	INTACT	35.66
	50	PED	INTACT	PED	INTACT	PED	18.62
	75	PED	INTACT	PED	INTACT	PED	7.04
8	25	INTACT	INTACT	INTACT	INTACT	FAILED	28.46
	50	INTACT	INTACT	INTACT	INTACT	FAILED	13.00
	75	INTACT	INTACT	PED	INTACT	PED	6.02
9	25	INTACT	INTACT	INTACT	INTACT	PED	27.77
	50	INTACT	INTACT	INTACT	INTACT	PED	10.55
	75	INTACT	INTACT	INTACT	INTACT	PED	5.24
10	25	INTACT	INTACT	INTACT	INTACT	INTACT	24.95
	50	INTACT	INTACT	INTACT	INTACT	INTACT	11.12
	75	INTACT	INTACT	INTACT	INTACT	INTACT	6.19

available resources is 5, we can see that the optimal retrofitting option is the following: (1) 25% pedestrian–75% cars: Bridges C and D should be intact (INTACT), and link E should be pedestrian accessible (PED); (2) 50% pedestrian–50% cars: Bridges B and D should be intact (INTACT), and bridge C should be pedestrian accessible (PED); and (3) 75% pedestrian–25% cars: Bridges A, B, and C should be pedestrian accessible (PED), and link E should be intact (INTACT). This is mostly because as the percentage of the pedestrians increases, having INTACT bridges loses its importance. Therefore, the rational decision would be to distribute the resources in a way to have more pedestrian accessible links and

bridges. From Table 3, it is obvious bridge C is the first one that should be retrofitted for most of the cases, followed by link E, bridge B, and bridge D. Among these 5 critical links, bridge A is the least likely to be retrofitted in most of the cases. Other *RATIO*s will result in fairly the same conclusion, but slightly different link prioritizations (Mostafizi 2016).

5 Discussion of implications for community planning

In this work, we created an agent-based modeling framework to systematically characterize the critical links of the transportation network as a result of an unplanned network disruption due to a CSZ/tsunami event. Results indicate that network failure severely impacts the mortality rate of the scenario and the efficiency of the evacuation. The criticality of a link is measured by the contribution of a particular link's failure to the overall mortality rate of the scenario. A set of critical links have been identified after a systematic characterization of each link's contribution to the overall mortality rate for different evacuation mode splits between driving and walking on foot. Each link' contribution is measured by the mortality rate when a specific link fails, while the rest of the links are intact in the scenario. The link importance defined in this context is relative in nature. The relative importance could be governed by the joint impacts from multiple different factors/parameters (i.e., mode split, walking or driving speeds, the existence of vertical evacuation structures). One link can be highly influential when one of the evacuation modes has the majority, but not when the other mode rules. After that, a mutual set of critical links of all the evacuation mode splits, informed by engineering judgment and structural criticality and vulnerability of the link, has been chosen for further retrofitting assessment.

The modeling framework has been applied to the city of Seaside, OR, as a case study. The results identified four bridges and one link as being the most critical—whose failure increases the mortality rates by great amounts. Then, a retrofitting plan has been created to minimize the number of fatalities considering the limited amount of retrofitting resources. The analysis incorporated the different levels of retrofitting (i.e., pedestrian accessible and intact). The results of the assessment of the city of Seaside transportation network have shown that neither all the bridges failures impact the mortality rate, nor all the critical links are the bridges. This research also captures the marginal mortality rate with the change in number of resources available to provide a baseline to assess further cost–benefit analyses. Furthermore, for the case of the city of Seaside, retrofitting schemes have shown that in most of the cases, bridge C should have the highest priority to be retrofitted, and after that, depending on the mode choice split, link E, bridge D, or bridge B are the next critical links, respectively.

6 Conclusion and future remarks

6.1 Summary of contributions and findings

The overall contribution of this study is the novel agent-based tsunami evacuation modeling framework which allows accurate modeling of unplanned network disruptions on the critical links in a transportation network. The characterization of each link's importance/contribution facilitates the creation of evidence-driven retrofitting strategies and resource allocation decision making to increase the overall network resilience through

informed and targeted proactive protection to those critical links. The major findings of this research are:

1. The agent-based modeling and simulation framework are uniquely situated to identify and characterize the criticality of each link through an iterative Monte Carlo approach.
2. The links in a transportation network are not equally significant in terms of each individual's contribution to the overall life safety outcomes measured by mortality rate. There exist links whose criticality to life safety is counterintuitive.
3. Diverse ways of spending the limited retrofitting resources can generate dramatically different life safety outcomes.
4. Accurate characterization and modeling of the unplanned network disruptions will facilitate the creation of evidence-driven retrofitting planning strategies and inform resource allocations that enhance network resilience.

These findings emphasize the importance of proactive evidence-driven retrofitting planning and informed resource allocation to enhance the network resilience especially considering that retrofitting resources are often inadequate. The agent-based tsunami evacuation modeling framework, as an integrated and interdisciplinary approach, is uniquely situated to merge transportation engineering, social science, and hazard science to address problems in a multi-hazard context (i.e., earthquake and tsunami). The results of our models provide baseline data that allows for future unplanned network disruption modeling research, as well as useful tools for local emergency planners and managers to identify social and infrastructure parameters unique to their locations and enhance community resiliency to a CSZ earthquake and near-field tsunami.

6.2 Future remarks

The presence of vertical evacuation shelters can dramatically change the criticality of a link. As an alternative, investing resources in building highly resistant shelter structures inside the inundation zone might be more economical than spending greater amounts of resources on retrofitting bridges or transportation links. Therefore, future work needs to incorporate the impact of having vertical evacuation shelters on vulnerability and criticality of the transportation network. Additionally, the creation of population distributions at different times of day (day of week), the number of tourists, and their combined effect on link criticality are beyond the scope of this study but will be assessed as a logical next step. In addition, social aspects of the evacuation scenario necessitate more extensive investigation. Population characteristics, coalescing behavior, car-abandoning (evacuation mode transfer) and communications (information provision and propagation strategies), and alternative daytime or nighttime contexts need to be considered in the future evacuation scenarios. Moreover, very likely, earthquake-induced damages could reduce the usability or capacity of facilities, but not necessarily to the extent to completely eliminate the use of a certain mode of transportation. Thus, capacity drop, as a consequence of earthquake damage to the transportation network, could serve as an alternative metric for network assessment. In addition, realistic interaction rules among agents (i.e., pedestrian and car interaction) to provide more accurate representation of the multimodal evacuation should be taken into consideration.

Acknowledgements The authors would like to acknowledge the funding support from the National Science Foundation through grant CMMI #1563618: "An Integrated Social Science and Agent-based Modeling Approach to Improve Life Safety from Near-field Tsunami Hazards" and Oregon Sea Grant program (#NA140AR4170064) through the project "Building resilient coastal communities: A social assessment of mobile technology for tsunami evacuation planning." Any opinions, findings, and conclusion or recommendations expressed in this research are those of the authors and do not necessarily reflect the view of the funding agencies.

References

Akiyama M, Frangopol DM, Arai M, Koshimura S (2012) Probabilistic assessment of structural performance of bridges under tsunami hazard. ASCE Struct Congr 1919–1928

Berdica K (2002) An introduction to road vulnerability: what has been done, is done and should be done. Transp Polic 9(2):117–127

Bocchini P, Frangopol DM (2010) Optimal resilience-and cost-based postdisaster intervention prioritization for bridges along a highway segment. J Bridg Eng 17(1):117–129

Brackstone M, McDonald M (1999) Car-following: a historical review. Transp Res F Traffic Psychol Behav 2(4):181–196

Chandler RE, Herman R, Montroll EW (1958) Traffic dynamics: studies in car following. Op Res 6(2):165–184

Chang L, Peng F, Ouyang Y, Elnashai AS, Spencer BF Jr (2012) Bridge seismic retrofit program planning to maximize postearthquake transportation network capacity. J Infrastruct Syst 18(2):75–88

Earnest DC (2011) Geographic distribution of disruptions in weighted complex networks: an agent-based model of the us air transportation network. Complex adaptive systems. In: AAAI fall symposium, pp 34–43

FEMA (2008) Guidelines for design of structures for vertical evacuation from tsunamis, Technical report, APPLIED TECHNOLOGY COUNCIL, 201 Redwood Shores Pkwy, Suite 240 Redwood City. California 94065

Fessel A, Oettmeier C, Döbereiner H.-G (2014) An analytical model for percolation in small link degree transportation networks. In: Proceedings of the 8th international conference on bioinspired information and communications technologies, pp 81–86

Gazis DC, Herman R, Rothery RW (1961) Nonlinear follow-the-leader models of traffic flow. Op Res 9(4):545–567

Goldfinger C, Nelson CH, Morey AE, Johnson JE, Patton JR, e.a. Karabanov E (2012) Turbidite event history—methods and implications for holocene paleoseismicity of the cascadia subduction zone. U.S. Geological Survey Professional Paper 1661F, 170

Gonzalez FI, Geist EL, Jaffe B, Kanoglu U, Mofjeld HO, Synolakis C, Titov VV, Arcas DR, Bellomo D, Carlton D, Horning T, Johnson J, Newman J, Parsons T, Peters R, Peterson CD, Priest G, Venturato A, Weber J, Wong FL, Yalciner A (2009) Probabilistic tsunami hazard assessment at seaside, oregon, for near- and far-field seismic sources. J Geophys Res. doi:10.1029/2008JC005132

He X, Liu H (2012) Modeling the day-to-day traffic evolution process after an unexpected network disruption. Transp Res B 46(1):50–71

Herman R, Montroll EW, Potts RB, Rothery RW (1959) Traffic dynamics: analysis of stability in car following. Op Res 7(1):86–106

Jenelius E, Mattsson LG (2012) Road network vulnerability analysis of area-covering disruptions: a grid-based approach with case study. Transp Res A Polic Pract 46(5):746–760

Jenelius E, Petersen T, Mattsson LG (2006) Importance and exposure in road network vulnerability analysis. Transp Res A Pol Pract 40(7):537–560

Jenelius E, Mattsson L.-G, Levinson D (2010) The traveler costs of unplanned transport network disruptions: an activity-based modeling approach. 1–34

Jonkman SN, Vrijling JK, Vrouwenvelder ACWM (2008) Methods for the estimation of loss of life due to floods: a literature review and a proposal for a new method. Nat Hazards 46:353–389

Kiremidjian A, Moore J, Fan YY, Yazlali O, Basoz N, Williams M (2007) Seismic risk assessment of transportation network systems. J Earthq Eng 11(3):371–382

Klugl F, Bazzan ALC (2012) Agent-based modeling and simulation. AI Mag 29–40

Knoblauch R, Pietrucha M, Nitzburg M (1995) Field studies of pedestrian walking speed and start-up time. Transp Res Rec 1538:27–38

Konduri KC, Pendyala RM, You D, Chiu Y.-C, Hickman M, Noh H, Gardner B, Waddell P, Wang L (2013) A network-sensitive transport modeling framework for evaluating impacts of network disruptions on traveler choices under varying levels of user information provision. In: 92nd Annual meeting of the Transportation Research Board, Washington, DC, p 510

Koshimura S, Katada T, Mofjeld HO, Kawata Y (2006) A method for estimating casualties due to the tsunami inundation flow. Nat Hazards 39(2):265–274

Lind N, Hartford D, Assaf H (2004) Hydrodynamic models of human stability in a flood. JAWRA J Am Water Resour As 40(1):89–96. doi:10.1111/j.1752-1688.2004.tb01012.x

Lindell MK, Prater CS (2007) Critical behavioral assumptions in evacuation time estimate analysis for private vehicles: examples from hurricane research and planning. J Urban Plan Devel 133(1):18–29

Mas E, Imamura F, Koshimura S (2011) Modeling the decision of evacuation from tsunami, based on human risk perception. In: Annual meeting of the Tohoku Branch Technology Research conference

Mas E, Suppasri A, Imamura F, Koshimura S (2012) Agent-based simulation of the 2011 great east Japan earthquake/tsunami evacuation: an integrated model of tsunami inundation and evacuation. J Nat Disaster Sci 34(1):41–57

Mas Erick FI, Koshimura S (2012) An agent-based model for the tsunami simulation: case study of the 2011 great east Japan tsunami in arahama town. Joint conference proceeding. In: 9th International conference on urban earthquake engineering & 4th Asia conference on earthquake engineering. Tokyo Institute of Technology, Tokyo, Japan

Miller HJ, Wu Y.-H, Hung M.-C (1999) Gis-based dynamic traffic congestion modeling to support time-critical logistics. In: Proceedings of the 32nd annual Hawaii international conference on systems sciences. HICSS-32

Mostafizi A (2016) Agent-based tsunami evacuation model : life safety and network resilience, Master's thesis, Oregon State University

Muhari A, Imamura F, Koshimura S, Post J (2011) Examination of three practical run-up models for assessing tsunami impact on highly populated areas. Nat Hazards Earth Syst Sci 11(12):3107–3123

Murray-Tuite P (2007) Perspectives for network management in response to unplanned disruptions. J Urban Plan Dev 133(1):9–17

Murray-Tuite P, Mahmassani HS (2005) Identification of vulnerable transportation infrastructure and household decision making under emergency evacuation conditions. No. SWUTC/05/167528-1, Southwest Region University Transportation Center, Center for Transportation Research, University of Texas at Austin

Naser M, Birst SC (2010) Mesoscopic evacuation modeling for small- to medium-sized metropolitan areas, Technical report, Advanced Traffic Analysis Center, Upper Great Plains Transportation Institute, North Dakota State University, Fargo, ND 58108

Pan X, Han CS, Dauber K, Law KH (2007) A multi-agent based framework for the simulation of human and social behaviors during emergency evacuations. AI Soc 22:113–132

Park H, Cox DT (2016) Probabilistic assessment of near-field tsunami hazards: inundation depth, velocity, momentum ux, arrival time, and duration applied to seaside, oregon. Coast Eng 117:79–96

Park S, van de Lindt JW, Gupta R, Cox D (2012) Method to determine the locations of tsunami vertical evacuation shelters. Nat Hazards 63(2):891–908

Priest GR, Stimely LL, Wood NJ, Madin IP, Watzig RJ (2016) Beat-the-wave evacuation mapping for tsunami hazards in seaside, Oregon, USA. Nat Hazards 80(2):1031–1056

Priest GR, Witter RC, Zhang YJ (2013) Tsunami animations, time histories, and digital point data for flow depth, elevation, and velocity for the South Coast Project Area, Curry County, Oregon, Technical Report Open-File Report O-13-13, Department of Geology and Mineral Industries

Qian ZS, Zhang HM (2013) Full closure or partial closure? Evaluation of construction plans for the i-5 closure in downtown Sacramento. J Transp Eng 139(3):273–286

Rahimian S, Mcneil S (2012) Post earthquake transportation network performance: transportation of injured to medical facilities. In: 2012 NZSEE conference, p 59

Railsback SF, Lytinen SL, Jackson SK (2006) Agent-based simulation platforms: review and development recommendations. Simulation 82(9):609–623

Satake K, Wang K, Atwater BF (2003) Fault slip and seismic moment of the 1700 Cascadia earthquake inferred from Japanese tsunami descriptions. J Geophys Res 108(B11):1978–2012

Schulz K (2015a) How to stay safe when the big one comes. http://www.newyorker.com/tech/elements/how-to-stay-safe-when-the-big-one-comes

Schulz K (2015b) The really big one, Annals of Seismology. http://www.newyorker.com/magazine/2015/07/20/the-really-big-one

Scott DM, Novak DC, Aultman-Hall L, Guo F (2006) Network robustness index: a new method for identifying critical links and evaluating the performance of transportation networks. J Transp Geogr 14(3):215–227

Sullivan JL, Aultman-Hall L, Novak DC (2009) A review of current practice in network disruption analysis and an assessment of the ability to account for isolating links in transportation networks. Transp Lett 1(4):271–280

Sullivan JL, Novak DC, Aultman-Hall L, Scott DM (2010) Identifying critical road segments and measuring system-wide robustness in transportation networks with isolating links: A link-based capacity-reduction approach. Transp Res A Polic Pract 44(5):323–336

Tatano H, Tsuchiya S (2008) A framework for economic loss estimation due to seismic transportation network disruption: a spatial computable general equilibrium approach. Nat Hazards 44(2):253–265

Thiele JC (2014) R marries NetLogo: introduction to the RNetLogo package. J Stat Softw 58(2):1–41

Thiele JC, Kurth W, Grimm V (2012) RNetLogo: an R package for running and exploring individual-based models implemented in NetLogo. Methods Ecol Evol 3(3):480–483

Titov VV, Gonzalez FI (1997) Implementation and testing of the method of splitting tsunami (MOST) model, Technical report, US Department of Commerce, National Oceanic and Atmospheric Administration, Environmental Research Laboratories, Pacific Marine Environmental Laboratory

TRB, Highway Capacity Manual, (2010) Transportation Research Board. National Research Council, Washington, D.C., p 2010

Tweedie SW, Rowland JR, Walsh SJ, Rhoten RP (1986) A methodology for estimating emergency evacuation times. Soc Sci J 23(2):189–204

Venturato AJ, Arcas D, Kanoglu U (2007) Modeling tsunami inundation from a Cascadia subduction zone earthquake for long beach and ocean shores, Washington, Technical report, National Oceanic and Atmospheric Administration, Seattle. WA, Pacific Marine Environmental Lab

Wang H, Mostafizi A, Cramer LA, Cox D, Park H (2016) An agent-based model of a multimodal near-field tsunami evacuation: decision-making and life safety. Transp Res C Emerg Technol 64:86–100

Wilensky U (1999) Netlogo. http://ccl.northwestern.edu/netlogo/. Center for connected learning and computer-based modeling, Northwestern University. Evanston, IL

Wood N (2007) Variations in city exposure and sensitivity to tsunami hazards in Oregon., Technical report 5283, U.S. Geological Survey Scientific Investigations Report

Wood NJ, Schmidtlein MC (2012) Anisotropic path modeling to assess pedestrian-evacuation potential from Cascadia-related tsunamis in the US Pacific Northwest. Nat Hazards 62(2):275–300

Wood NJ, Schmidtlein MC (2013) Community variations in population exposure to near-field tsunami hazards as a function of pedestrian travel time to safety. Nat Hazards 65(3):1603–1628

Wood NJ, Jones J, Spielman S, Schmidtlein MC (2016) Community clusters of tsunami vulnerability in the us pacific northwest. Proc Nat Acad Sci 112(17):5354–5359

Wood N, Jones J, Schelling J, Schmidtlein M (2014) Tsunami vertical-evacuation planning in the US Pacific Northwest as a geospatial, multi-criteria decision problem. Int J Disaster Risk Reduct 9:68–83

Xie F, Levinson D (2011) Evaluating the effects of the i-35w bridge collapse on road-users in the twin cities metropolitan region. Transp Plan Technol 34(7):691–703

Yeh H (2010) Gender and age factors in tsunami casualties. Nat Hazards Rev 11(1):29–34

Yin W, Murray-Tuite P, Ukkusuri SV, Gladwin H (2014) An agent-based modeling system for travel demand simulation for hurricane evacuation. Transp Res C Emerg Technol 42:44–59

Zhu S, Levinson DM (2012) Disruptions to transportation networks: a review. Network reliability in practice. Springer, New York

Zhu S, Levinson D, Liu HX, Harder K (2010) The traffic and behavioral effects of the i-35w Mississippi river bridge collapse. Transp Res A Polic Pract 44(10):771–784